ELSEVIER

Biophysical Chemistry 61 (1996) 1–7

Biophysical Chemistry

Emergent properties of coupled enzyme reaction systems 1. Switching and clustering behaviour

Baltazar D. Aguda

Department of Chemistry and Biochemistry, Laurentian University, Sudbury, Ont., Canada P3E 2C6

Received 20 June 1995; revised 30 January 1996; accepted 2 February 1996

Abstract

The dynamics of locally and globally coupled cells that convert a substrate to a product via an uncompetitive substrate-inhibition mechanism is studied. When the cell–cell coupling strength is below a threshold value, the coupled system exhibits a large number of steady states; however, all cells cluster to one state when coupling exceeds the threshold value. The coupled system also exhibits a buffering capacity that maintains low and almost constant intracellular and extracellular substrate levels; however, there exists a threshold value on the influx rate of extracellular substrate beyond which the system switches to higher substrate levels. This transition becomes sharper as the number of coupled cells increases. Propagation failure of concentration fronts between adjacent cells is also exhibited by the system.

Keywords: Coupled enzyme system; Substrate-inhibition kinetics; Bistability; Clustering; Propagation failure; Computer simulation

1. Introduction

In the biochemical machinery of the living cell, enzymes play a crucial role in determining which reaction pathways are implemented. Several pathways are often intricately intertwined to form large networks of enzymatic reactions with resulting dynamics that remains to be studied systematically. Some examples of kinetic behaviour that emerge from these complex systems include glycolytic oscillations [1], intracellular Ca^{2+} and cAMP oscillations [2], switching behaviour in coupled cyclic enzyme systems as in the phosphotransferase system [3], and behaviour reminiscent of neurons and computer logic gates [4].

The next level in the hierarchy of complexity in an organism involves cell–cell interactions as well as interactions with the surrounding medium. When cells interact indirectly with other cells through a common pool of substances (in other words, each cell affects this pool which in turn affects the other cells), we say that the cells have global coupling. Interactions between adjacent cells will be referred to as local coupling. A demonstration of local coupling between cells would be the experiments involving culture cells grown on a glass or plastic surface where it was observed that cell division is inhibited as soon as the cells form a continuous monolayer and division is resumed for those cells whose immediate neighbors are taken out [5]. An interesting example of the effect of global coupling would be the experiments on *E. coli* cells suspended in a liquid culture and interacting globally through a common medium [6]; in these experiments, it was found that cell differentiation occurs without spatial or positional information but was induced by suffi-

PII S0301-4622(96)00019-1

cient nutrient levels. Kaneko and Yomo [7] have since proposed a novel mechanism of cell differentiation based on dynamic clustering as a result of global coupling. Mizuguchi and Sano [8] also proposed a simple model that describes the regulation, by global coupling, of the proportion of two cell types resulting from the differentiation of slime mold cells. All the models mentioned above, however, use over-simplified or even abstract reaction mechanisms to describe the enzyme dynamics.

In this paper, we present the results of our study on the effect of global and local coupling in a population of "chemical cells" where each cell converts a substrate to a product through an enzymatic reaction characterized by inhibition kinetics. We first consider in Section 2 various types of enzyme-inhibition kinetics and decide which among these will exhibit bistability. Bistability is the coexistence, under the same set of parameters, of two stable steady states. We expect that bistable kinetics will help us explain various switching behaviours in biochemical systems. Among the mechanisms analyzed in Section 2, only the uncompetitive substrate-inhibition (USI) type supports bistability and we therefore use this mechanism in the computer simulations of the behaviour of a community of cells which are coupled globally and/or locally. The procedure used in the computer simulation is described in Section 3 and the results are presented in Section 4 and Section 5. We give our conclusions in Section 6.

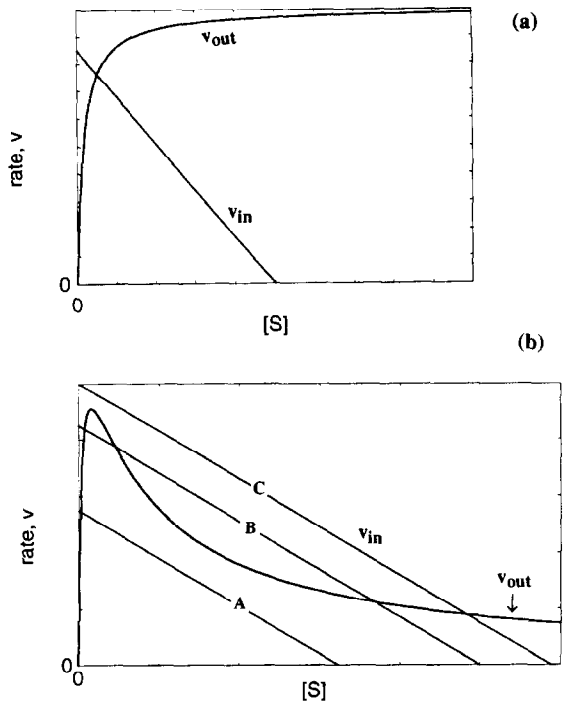

Fig. 1. Steady-state rates (v_{out} curves) as functions of substrate concentrations for the (a) Michaelis–Menten mechanism, and (b) uncompetitive substrate-inhibition mechanism. The lines labelled v_{in} represent the net influx rate of substrate from an external medium according to the equation $v_{in} = k_1[S_0] - k_{-1}[S]$. The number of intersections between the curves v_{out} and v_{in} gives the number of steady states of S.

2. Enzyme inhibition mechanism and bistability

In closed systems, a chemical reaction eventually goes to a unique equilibrium state. However, under open conditions (as in a flow reactor), several stable non-equilibrium steady states can coexist under the same set of parameters. The Michaelis–Menten (MM) mechanism, shown below, by itself cannot generate multiple steady states no matter how far it is driven away from equilibrium. This is because the steady state rate law is a hyperbolic function of [S] (see curve v_{out} in Fig. 1(a)).

MM Mechanism:

$S + E \rightleftharpoons ES \rightarrow E + P$

If, however, the substrate S undergoes an autocatalytic reaction, for example by reacting with a species A as in $A + S \rightleftharpoons 2S$, then this reaction coupled with the MM mechanism will give rise to bistability as was demonstrated by Edelstein [9].

Let us now consider only enzyme inhibition mechanisms with non-autocatalytic substrates. We analyze the four types that were studied by Roussel and Fraser [10] given in the table below:

Inhibition Type	Step Added to MM mechanism
Competitive inhibition (CI)	$I + E \rightleftharpoons EI$
Competitive substrate inhibition (CSI)	$S + E \rightleftharpoons ES'$
Uncompetitive inhibition (UI)	$I + ES \rightleftharpoons IES$
Uncompetitive substrate inhibition (USI)	$S + ES \rightleftharpoons SES$

In the table above, EI, ES′, IES and SES are dead-end enzyme-substrate complexes and I is an inhibitor different from S.

It can be shown (see for example Ref. [11]) that mechanisms CI, CSI and UI give hyperbolic rate laws similar to the curve labelled v_{out} in Fig. 1(a). In contrast, mechanism USI gives a non-hyperbolic rate law as shown by the curve v_{out} in Fig. 1(b). If the system is open to an influx of substrate as represented by the pseudo-reaction $\{S_0 \rightleftharpoons S\}$ where S_0 is some pool of substrate, the net influx rate of S is given by $v_{in} = k_1[S_0] - k_{-1}[S]$. As shown graphically in Fig. 1(b), three steady-state concentrations for S are possible: when v_{in} intersects v_{out} three times as in the case of line B in the figure. We have already worked out the exact conditions for the existence of three steady states for the USI mechanism and the results have been published [12]. (These results are derived from an exact analysis of the geometry of the cusp catastrophe manifold; see Eq. (4.3) of Ref. [12]). Consider the USI mechanism including the influx of substrate: $S_0 \overset{1}{\underset{-1}{\rightleftharpoons}} S$, $S + E \overset{2}{\rightarrow} ES$, $ES \overset{3}{\rightarrow} E + P$, $S + ES \overset{4}{\underset{-4}{\rightleftharpoons}} SES$. The necessary conditions for the existence of three steady states are [12]:

$$\left(\frac{k_1 S_0}{k_{-1}}\right) > \left(\frac{k_{-4}}{k_4}\right) \tag{1}$$

$$E_{total} > \frac{k_1 S_0}{k_3} - \frac{k_{-1}}{k_2} \tag{2}$$

The parameters used in Fig. 3 satisfy the above inequalities: stability analysis of the three steady states shows that two are stable and the middle steady state is unstable. Initial conditions will determine which of the two stable steady states is reached.

3. Computer simulation of coupled USI cells

We now envisage a situation in which an enzyme reaction with a USI mechanism occurs inside a cell bounded by a membrane that is permeable to a substrate S. A ring of n cells is immersed in a bath with extracellular substrate concentration $[S_0]$. Each cell exchanges substrate with the bath and with its adjacent neighbors through discrete diffusion (see Fig. 2). Each cell i has four dynamical species, namely S_i, E_i, ES_i, and SES_i, with concentrations changing in time according to the following set of differential equations:

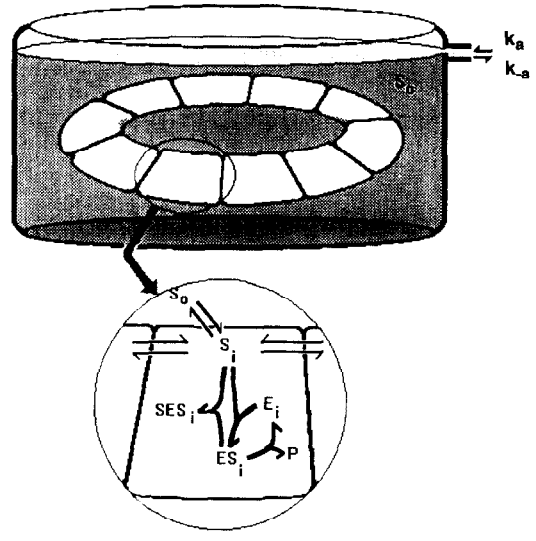

Fig. 2. The dynamics of the above system of coupled cells is simulated in a computer. A ring of cells is immersed in a well-stirred medium with substrate concentration S_0. Each cell converts the intracellular substrate S_i to product P via an uncompetitive substrate-inhibition mechanism shown in the magnification of one cell. Each cell is globally coupled to all the others through S_0. Local coupling between adjacent cells is through discrete diffusion of intracellular substrate.

$$\frac{d[S_i]}{dt} = k_1[S_0] - k_{-1}[S_i] - k_2[S_i][E_i] - k_4[S_i][ES_i] + k_{-4}[SES_i] + K\{[S_{i+1}] - 2[S_i] + [S_{i-1}]\} \tag{3a}$$

$$\frac{d[E_i]}{dt} = -k_2[S_i][E_i] + k_3[ES_i] \tag{3b}$$

$$\frac{d[ES_i]}{dt} = k_2[S_i][E_i] - k_3[ES_i] - k_4[S_i][ES_i] + k_{-4}[SES_i] \tag{3c}$$

$$\frac{d[SES_i]}{dt} = k_4[S_i][ES_i] - k_{-4}[SES_i] \tag{3d}$$

One additional differential equation describes the kinetics of the extracellular substrate S_o:

$$\frac{d[S_o]}{dt} = (k_a - k_{-a}[S_o]) - \sum_{i=1}^{n} (k_1[S_o] - k_{-1}[S_i]) \quad (3e)$$

For simplicity, we assume that the rate constant for a given reaction is identical in all cells. It is also assumed that the product P of the enzymatic reaction is not a dynamical species and does not affect the kinetics of the reaction. In Eq. (3a), the constant K is referred to as the cell–cell coupling constant. The set of differential equations (Eqs. (3a), (3b), (3c), (3d) and (3e)) was integrated using the routine LSODE [13].

4. Regulation and switching of substrate levels

It is instructive to first look at the intrinsic dynamics of a single cell exposed to progressively increasing extracellular substrate concentration. In Fig. 3(a), the steady state concentrations $[S]_{ss}$ and $[S_o]_{ss}$ are plotted against the parameter k_a which is the rate of input of S_o (see Fig. 2). Initially the values of $[S]_{ss}$ and $[S_o]_{ss}$ are maintained at low levels; however, beyond a critical value k_a^*, $[S]_{ss}$ and $[S_o]_{ss}$ increase sharply. This transition can be explained with the aid of Fig. 1(b): for $k_a < k_a^*$, the rate of intake of substrate into the cell, v_{in}, corresponds to line A in Fig. 1(b); this line intersects v_{out} to give a small value of $[S]_{ss}$. As k_a is increased, the y intercept of the v_{in} line increases (its slope remaining constant) until the three-steady-state region is reached (see, for example, Fig. 1 line B). Beyond k_a^*, a sudden increase in the observed $[S]_{ss}$ occurs because we then have the case shown by Fig. 1 line C where only the high steady state exists.

How does the particular behaviour of a single cell described in the preceding paragraph carry over to a community of cells depicted in Fig. 2? When we repeated the simulation with two cells, the value of k_a^* increases to 25 compared to 17 for a single cell; furthermore, the increase in $[S]_{ss}$ and $[S_o]_{ss}$ at k_a^* is steeper. In Fig. 3(b), we show the results of a simulation involving 10 cells with only global coupling, i.e. the cells share the extracellular substrate S_o and no cell–cell exchange is allowed. It is assumed that the cell environment is well-stirred and therefore the extracellular medium is homogeneous in S_o. First, we see in Fig. 3(b) that k_a^* has now increased to 93.9 which is about 5.5 times the value for a single cell and, second, the intracellular and extracellular substrate levels for $k_a > k_a^*$ are now almost an order of magnitude higher than those of the single-cell system. Note that the substrate levels, both intracellular and extracellular, are maintained at fairly constant low values for $k_a < k_a^*$; we say that the community of cells possesses a buffering capacity.

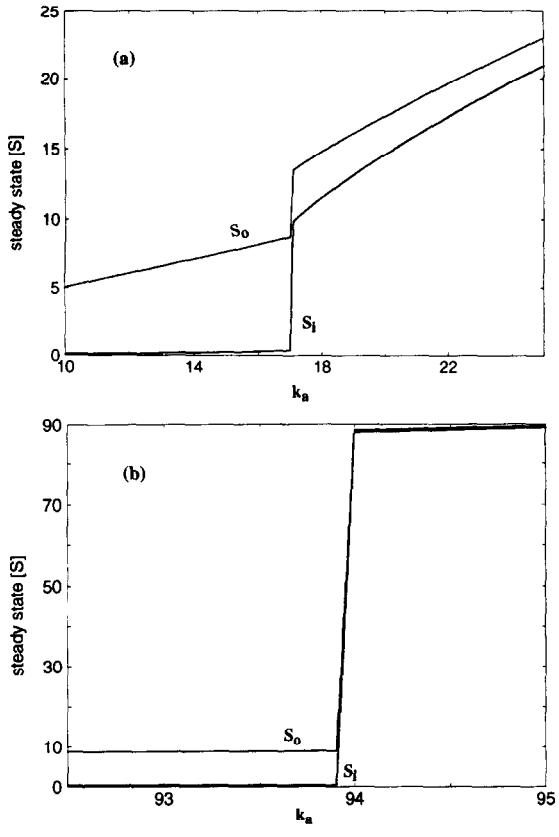

Fig. 3. Steady state concentrations of extracellular substrate, S_o, and intracellular substrate, S_i, versus the influx rate, k_a, of S_o for a system with (a) one cell, and (b) ten cells as shown in Fig. 2. Parameter values used are: $k_1 = k_{-1} = 1.0$, $k_2 = 20.0$, $k_3 = 3.0$, $k_4 = 1.0$, $k_{-4} = 4.0$, $k_{-a} = 1.0$. No cell-cell coupling is introduced in (b). Initial conditions for (a): $[S_o] = 10$, $[S_i] = 4$, $[E_i] = 0.2$, $[ES_i] = 3$, $[SES_i] = 1$. Initial conditions for (b): $[S_o] = 10$, for the ten cells: $([S_i],[E_i],[ES_i],[SES_i]) = (4,0.2,3,1)$, $(3.8,0.2,2,2)$, $(3.6,0.5,3.2,0.5)$, $(3.4,1,2,1.2)$, $(3.2,1.2,1.5,1.5)$, $(0.2,4.2,0,0)$, $(0.4,4.2,0,0)$, $(0.6, 4.2,0,0)$, $(0.8,4.2,0,0)$, $(1,4.2,0,0)$.

The presence of cell–cell coupling does not change the qualitative appearance of Fig. 3(b). This local coupling merely shifts the value of k_a^* to larger values; for example, when the cell–cell coupling constant $K = 10$, k_a^* increases to about 100 for 10 cells. As the value of K is increased further, k_a^* asymptotically reaches a value of about 100.7 (we verified this for values of $K = 20$–500); also, for k_a just above k_a^*, the value of $[S]_{ss}$ approaches a value of about 96 as K goes to 500).

When the number of cells is increased to 20, the results of the simulations are qualitatively similar to that shown in Fig. 3(b) but the value of k_a^* significantly increases to 188.8; moreover, right after the transition, the substrate levels increase to about 180. The increase in k_a^* with increasing number of cells is to be expected because all cells share the same extracellular medium. The increase in the substrate levels after the transition as the cell number is increased is also not surprising considering the fact that the inflow rate for S_0 has increased (i.e. increased k_a^*) which leads to higher substrate levels once the system has gone beyond its buffering capacity.

We emphasize that the value of k_a^* depends on the initial conditions. For example, if the initial intracellular substrate concentration of cell 2 is decreased from 3.8 to 0.8 (see caption of Fig. 3(b)) then k_a^* increases from 93.9 to 95.7.

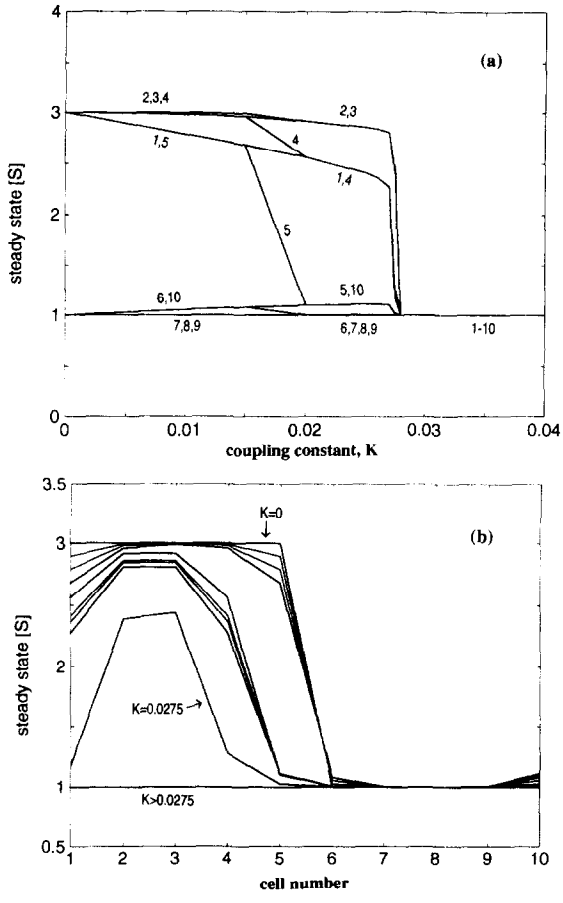

Fig. 4. (a) Steady state concentrations of intracellular substrates as a function of cell–cell coupling constant, K, for the set of initial conditions given in Fig. 3(b). When $K = 0$, cells 1–5 go to the higher state, $[S]_{ss} = 3$, while cells 6–10 go to the lower state, $[S]_{ss} = 1$. The numbers beside the various curves indicate the cell number. Parameter values used are identical to those of Fig. 3 except $k_1[S_0] = 10$ here (S_0 is assumed constant). (b) Steady state concentration profiles for the various cell–cell coupling constants corresponding to the data plotted in (a).

5. Clustering and propagation failure

Another computer experiment was performed using a ring of 10 cells and parameter values that will give bistability for each isolated cell. Initial conditions are such that, when no cell–cell coupling is introduced, five adjacent cells go to the high stable $[S]_{ss}$ while the other five adjacent cells go to the low stable $[S]_{ss}$. In the experiment shown in Fig. 4(a), $[S_0]$ is not a dynamical variable but is kept constant while the cell–cell coupling constant K is increased slowly. At each value of K, integration of the kinetic equations (Eqs. (3a), (3b), (3c), (3d) and (3e)) start at the initial conditions used for the $K = 0$ case (no cell–cell coupling) and the intracellular substrate concentrations are determined after 1000 time units (which is more than sufficient for all other species to attain steady state). We see in Fig. 4(a) that various steady states emanate from the two stable steady states of the $K = 0$ case. The coupled system gives rise to a high multiplicity of steady states; which of these steady states is reached depends sensitively on the initial conditions. As can be seen in Fig. 4(a), these steady states are grouped into two, each group associated with the original non-coupled stable steady states. We note that beyond a certain threshold value of the cell–cell coupling constant, namely $K_c \approx$

0.0275, all the cells go to the lower stable $[S]_{ss}$. Fig. 4(b) shows the profile of the intracellular steady-state substrate concentrations versus cell number for various K. As long as $K < K_c$, these steady-state profiles are stable; in other words, unlike diffusion in continuous media, there is a failure in the propagation of a concentration front between adjacent cells.

We emphasize that the steady state profiles for various K values depend on initial conditions. The threshold value K_c was also observed to depend on initial conditions.

How can we explain the existence of a threshold value K_c? The root cause of this threshold phenomenon is again explained by referring to Fig. 1(b). If the cell–cell coupling is increased, the magnitudes of the slope and y intercept of the v_{in} line is increased; so, for example, line B (which is associated with three steady states) is shifted to the left with steeper slope and higher y intercept until the three intersections with the v_{out} curve is reduced to just one corresponding to the low $[S]_{ss}$.

Cells with different steady states $[S]_{ss}$ can be considered to be of different types. The phenomenon involving one type of cell differentiating into two types can also be observed when the cell–cell coupling constant K is decreased from a high value to one that is lower than K_c. The proportions of cells going to the two stable states depend on the initial conditions.

6. Conclusions

We have considered a few simple enzyme inhibition mechanisms and showed that the USI-type gives rise to bistability. Computer simulations were performed to study the dynamics of a community of cells, each cell converting a substrate S to the product P via the USI enzyme pathway. One interesting result is the cooperative behaviour of the cells in maintaining low concentration levels of the substrate both inside and outside the cells; however, this buffering capacity breaks down suddenly beyond a threshold value of the extracellular substrate concentration (corresponding to a threshold value of the input rate k_a^*). The switching behaviour of the system, i.e. the transition from low substrate concentrations to high concentrations, becomes more pronounced as the number of cells increase. This phenomenon is similar to the neuron-like behaviour of coupled cyclic enzyme systems studied by Okamoto and co-workers [3,14].

Coupling of the bistable USI cells has been shown to lead to a large number of steady states of the system. This result agrees with a recently reported theorem due to MacKay and Sepulchre [15] on the existence of a high degree of multiplicity of stable steady states in a system of weakly coupled bistable units with very general inter-unit coupling. We have also demonstrated another claim of this theorem, namely, that there is a smooth continuation of the steady states from the uncoupled case to the steady states of the coupled system.

The number of steady states of the coupled system is basically dictated by the intrinsic bistability of each cell. We have seen that there is a threshold value for the degree of cell–cell coupling below which two clusters of cells exist depending on the initial conditions and above which only one cluster is formed.

Another property exhibited by the coupled bistable cells is the propagation failure of a concentration front between cells when the degree of cell–cell coupling is weak. Laplante and Erneux [16] have also demonstrated this phenomenon in their experiments involving coupled bistable chlorite–iodide reactions. Keener [17] has shown mathematically that propagation failure is a property of the discrete system and cannot be observed in a one-variable continuous reaction-diffusion system if the parameters are uniformly distributed; however, if the parameters are not uniform throughout the continuous medium, propagation failure is possible.

There are many other ways that we can couple the cells together but we have only studied the effects of discrete diffusion of substrate between cells. An example of richer dynamics still to be explored is the possibility of inducing concentration oscillations when bistable cells are coupled in the right way (see for example, Ref. [18]).

Lastly, we comment on a similarity between the mechanism of pattern formation in the discrete-diffusion system treated in this paper and in a continuous system undergoing Turing instability [19]. In the latter, under certain conditions, two interacting chemicals can generate stable stationary inhomoge-

neous patterns when one species (the inhibitor) diffuses faster than the other species (the activator). In the case of the ring of cells we studied in this paper, all of the enzyme species in each cell do not diffuse across the cell boundary and this non-diffusion ultimately contributes to the failure in the propagation of a concentration front as demonstrated in this paper.

Acknowledgements

This work is supported by a research grant from the Natural Sciences and Engineering Research Council of Canada.

References

[1] E. E. Sel'kov, Eur. J. Biochem., 4 (1968) 79.
[2] D.M.F. Cooper, N. Mons and J.W. Karpen, Nature, 374 (1995) 421.
[3] M. Okamoto and K. Hayashi, J. Theor. Biol., 113 (1985) 785.
[4] A. Hjelmfelt, E.D. Weinberger and J. Ross, Proc. Natl. Acad. Sci. USA, 88 (1991) 10983.
[5] S. L. Wolfe, Molecular and Cellular Biology, Wadsworth, 1993, p. 919.
[6] E. Ko, T. Yomo and I. Urabe, Phys. D, 75 (1994) 81.
[7] K. Kaneko and T. Yomo, Phys. D, 75 (1994) 89.
[8] T. Mizuguchi and M. Sano, Proportion Regulation in Globally Coupled Nonlinear Systems, preprint, 1995.
[9] B.J. Edelstein, J. Theor. Biol., 29 (1970) 57.
[10] M.R. Roussel and S.J. Fraser, J. Phys. Chem., 97 (1993) 8316.
[11] J. Tze-Fei Wong, Kinetics of Enzyme Mechanisms, Academic Press, 1975, p. 40, 55.
[12] B.D. Aguda and B.L. Clarke, J. Chem. Phys., 87 (1987) 3461.
[13] A. C. Hindmarsh, ACM Signum Newslett., 15 (1980) 10.
[14] M. Okamoto, T. Sakai and K. Hayashi, Biol. Cybernet., 58 (1988) 295.
[15] R.S. MacKay and J.-A. Sepulchre, Phys. D, 82 (1995) 243.
[16] J.P. Laplante and T. Erneux, J. Phys. Chem., 96 (1992) 4931.
[17] J.P. Keener, SIAM J. Appl. Math., 47 (1987) 556.
[18] M. Boukalouch, J. Elezgaray, A. Arneodo, J. Boissonade and P. De Kepper, J. Phys. Chem., 91 (1987) 5843.
[19] A.M. Turing, Trans. Philos. R. Soc. London Ser. B, 237 (1952) 37.